Biotechnology and Bioengineering

WILEY

BIOTECHNOLOGY AND BIOENGINEERING

ARTICLE OPEN ACCESS

Quantitative Analysis Reveals Hitchhiking Drives Polysorbate Hydrolase Persistence Via Host Cell Protein–Antibody Interactions

Melanie Maier[1,2] | Lukas Griesinger[1,2] | Matthias Franzreb[2] | Simon Kluters[1]

[1]Drug Substance Development Biologicals, Boehringer Ingelheim Pharma GmbH & Co.KG, Biberach an der Riss, Germany | [2]Institute of Functional Interfaces, Karlsruhe Institute of Technology, Karlsruhe, Germany

Correspondence: Simon Kluters (simon.kluters@boehringer-ingelheim.com)

Received: 9 December 2025 | **Revised:** 23 January 2026 | **Accepted:** 28 January 2026

Funding: Boehringer Ingelheim Pharma GmbH & Co. KG

Keywords: biolayer interferometry | downstream processing | hitchhiking | host cell proteins (HCPs) | monoclonal antibodies | polysorbate degradation

ABSTRACT

Polysorbate-degrading host cell proteins (HCPs) represent a critical challenge in the manufacturing of monoclonal antibody therapeutics due to their potential to persist during downstream processing. While their enzymatic activity has been characterized, the role of direct HCP-mAb interactions, particularly those involving polysorbate degrading HCPs, remains poorly understood. In this study, we systematically investigated the binding behavior of four representative polysorbate-degrading HCPs (CES1F, LPLA2, PAF-AH, and PPT1) to a panel of mAbs using biolayer interferometry (BLI). All tested HCPs showed specific, transient interactions characterized by fast-on/fast-off kinetics, with apparent equilibrium dissociation constants (K_D) in the low nanomolar range (40–90 nM for strong binders) and rapid dissociation kinetics ($k_d > 0.01\ s^{-1}$). This indicates a binding mode characterized by relatively high affinity but limited kinetic stability. Due to incomplete saturation and partially not meeting the quality criteria for kinetic fitting, we complemented model-based analysis with equilibrium-derived descriptors. The initial slope of the binding isotherm correlated well with kinetic parameters and enabled robust ranking of interaction strength. To assess hitchhiking relevance during downstream processing, we performed a Protein A chromatography experiment using PLBL2 as a model HCP and two mAbs with different interaction profiles. PLBL2 levels in Protein A elution pools correlated well with interaction propensity confirming that transient interactions can contribute to HCP co-elution. Our results provide the first systematic and quantitative comparison of polysorbate hydrolase–antibody interactions. They also demonstrate that direct mAb–HCP interaction is a relevant mechanism contributing to HCP persistence during downstream processing.

1 | Introduction

Polysorbates, such as PS20 and PS80, are commonly used in monoclonal antibody (mAb) formulations to prevent aggregation induced by interfacial stress and to ensure long-term stability of biopharmaceutical products (Kerwin 2008; Kishore et al. 2011). However, polysorbates are susceptible to degradation via oxidative and hydrolytic pathways, resulting in the formation of free fatty acids and visible or subvisible particles (Dwivedi et al. 2018; Jones

Abbreviations: BLI, biolayer interferometry; CES1F, carboxylesterase 1 f; CHO, Chinese hamster ovary; DNA, deoxyribonucleic acid; DSP, downstream processing; ELISA, enzyme-linked immunosorbent assay; Fab, fragment antigen binding; Fc, fragment crystallizable; HCP, host cell protein; HEPES, 4-(2-hydroxyethyl)-1-piperazineethanesulfonic acid; IgG, immunoglobulin G; LPLA2, lysosomal phospholipase A2; MS, mass spectrometry; MST, microscale thermophoresis; NSB, non-specific binding; pI, isoelectric point; PLBL2, putative phospholipase B-like 2; PPT1, palmitoyl-protein thioesterase 1; PS, polysorbate; QSPR, quantitative structure property relationship; SAX, high precision streptavidin (BLI-biosensor); SEC, size exclusion chromatography; SPR, surface plasmon resonance.

et al. 2018). Enzymatic hydrolysis mediated by host cell proteins (HCPs) is among these mechanisms and has emerged as a critical risk factor for product quality of biopharmaceutical formulations (Felix et al. 2025). Even at trace levels, polysorbate-degrading hydrolases can remain catalytically active (Hall et al. 2016; Tsukidate et al. 2024). Several hydrolases have been confirmed to degrade polysorbates under formulation-relevant conditions, including CES1F, CES2C, LPLA2, PAF-AH, PPT1, and LIPA (Felix et al. 2025; Kovner et al. 2023; Maier et al. 2024b). PLBL2, long considered active against polysorbate, was shown by knockout studies to lack polysorbate-degrading activity, although it frequently co-purifies with mAbs (Tran et al. 2016; Zhang et al. 2020).

Despite extensive efforts to characterize polysorbate-degrading enzymes in Chinese hamster ovary (CHO) cell-derived biotherapeutics (Kovner et al. 2023; Maier et al. 2024b), the mechanisms underlying their persistence during downstream processing remain poorly understood. Previous studies showed co-elution driven by physicochemical similarity between HCPs and mAbs during chromatographic separation (Levy et al. 2016; Maier et al. 2024a). Other studies suggest that weak, reversible protein-protein interactions may enable certain HCPs to "hitchhike" on therapeutic antibodies throughout purification (Aboulaich et al. 2014; Hecht et al. 2022; Oh et al. 2023). This poses a significant challenge for downstream purification strategies, as hitchhiking behavior is highly product specific and difficult to predict.

Characterizing these interactions is technically challenging because they are typically low-affinity, transient, and occur at sub-ppm concentrations. Previous attempts using surface plasmon resonance (SPR) and microscale thermophoresis (MST) reported limited sensitivity and high variability, leaving the interaction landscape largely unexplored (Hecht et al. 2022). Mass spectrometry and oxidative labeling offered structural insights but lack throughput for systematic screening (Hecht et al. 2022). Consequently, no broadly applicable platform exists for profiling HCP–mAb interactions.

Biolayer interferometry (BLI) is a label-free optical biosensing technique that enables real-time kinetic analysis with high sensitivity. It also supports the parallel screening of multiple interactions. While BLI has been widely applied in antibody discovery and epitope binning (Bates et al. 2025; Petersen 2017), its potential for detecting weak, reversible HCP–mAb interactions has, to the best of our knowledge, not been reported to date. This study addresses this gap by developing a BLI-based assay tailored to detect weak, reversible interactions between mAbs and polysorbate-degrading HCPs.

We systematically screened four representative polysorbate hydrolases (CES1F, LPLA2, PAF-AH, and PPT1) against eight model antibodies. To evaluate the relevance of these findings for downstream processing, we performed a Protein A chromatography experiment using PLBL2 as a model HCP. Our results provide the first systematic dataset linking HCP–mAb interaction strength to downstream persistence and highlight the potential of quantitative interaction profiling for early risk assessment of biologics development.

2 | Materials and Methods

2.1 | Model Antibodies

In this study, eight different model antibodies were used (Table 1). All model antibodies were produced in-house by Boehringer Ingelheim Pharma GmbH & Co. KG. The theoretical isoelectric point (pI) of each antibody was calculated based on its amino acid sequence.

TABLE 1 | Subtype and theoretical pI of model antibodies.

Antibody	Subtype	pI
mAb-1	IgG1	9.1
mAb-2	IgG1	8.9
mAb-3	IgG4	7.8
mAb-4	IgG4	7.8
mAb-5	IgG1	9.6
mAb-6	IgG1	8.8
mAb-7	IgG1	9.2
mAb-8	IgG1	7.9

2.2 | Expression and Purification of Recombinant HCPs

Hydrolases were recombinantly expressed using a transposase-based system. The coding sequences were derived from the CHO K1 transcriptome and cloned into a transposon-based expression plasmid. After transfection and selection, stable cell pools were cultivated, and recombinant proteins were purified from the harvested cell culture supernatant. Purification was performed using a three-step chromatographic protocol on an ÄKTA Avant 25 system (Cytiva Life Sciences, Marlborough, USA), comprising immobilized metal affinity chromatography (HisTrap FF crude, Cytiva Life Sciences, Marlborough, USA), Strep-Tactin affinity chromatography (StrepTrap XT, Cytiva Life Sciences, Marlborough, USA), and size exclusion chromatography (HiLoad Superdex 200, Cytiva Life Sciences, Marlborough, USA) for final polishing. Monomeric fractions were pooled, aliquoted, and stored at −70°C. Further details on the expression and purification strategy have been described previously (Maier et al. 2024b). HCPs included in this study are listed in Table 2.

2.3 | Biotinylation of Proteins

Ligand biotinylation was performed with EZ-Link NHS-PEG4-biotin (Thermo Fisher Scientific, Waltham, USA) to target solvent-accessible primary amines. A 20 mM stock solution was freshly prepared in deionized water and diluted to 0.2 mM for use. The proteins were adjusted to 1 mg/mL and the reagent was added to achieve a 3:1 molar coupling ratio (biotin:protein). The reaction was processed for 30 min with gentle mixing. Excess reagent was removed using Zeba 7 K MWCO spin desalting columns (Thermo Fisher Scientific, Waltham, USA).

2.4 | BLI Based Interaction Assay Development

Several Octet biosensor formats and assay orientations were initially evaluated. These included Fc-mediated antibody capture using Octet ProtA and Octet AHC Biosensors, as well as His-tag-based immobilization of recombinant HCPs on Octet HIS2 Biosensors (Sartorius, Göttingen, Germany). However,

TABLE 2 | HCPs selected for interaction studies, including pI, molecular weight (MW), and UniProt accession.

HCP	Abbreviation	Gene name	pI	MW (kDa)	Uniprot accession
Carboxylesterase 1 f	CES1F	*Ces1f*	7.9	65	A0A061I7X9
Group XV phospholipase A2	LPLA2	*Pla2g15*	6.3	50	G3HKV9
Platelet-activating factor acetylhydrolase	PAF-AH	*Pla2g7*	8.6	52	A0A8C2M2A7
Palmitoyl-protein thioesterase	PPT1	*Ppt1*	8.0	37	G3HN89
Phospholipase B-like 2	PLBL2	*Plbd2*	5.9	66	G3I6T1

these approaches were found unsuitable due to unstable baselines and high non-specific binding (NSB). The most robust configuration was achieved using biotinylated HCPs immobilized on Octet High Precision Streptavidin (SAX) Biosensors (Sartorius, Göttingen, Germany), combined with monoclonal antibodies as analytes in solution.

Ligand loading scouts were performed for each biotinylated HCP to identify the lowest concentration ensuring stable immobilization and sufficient signal. A two-fold dilution series from 40 to 1.25 μg/mL was tested under standard assay conditions using a fixed analyte concentration. Sensorgrams were reviewed for stable loading without overshoot, minimal baseline drift, and clear association and dissociation phases.

All experiments were performed on an Octet HTX system (Sartorius, Göttingen, Germany) in 384-well plates with 80 μL per well. Data acquisition and analysis were conducted using Octet BLI Discovery 13.0 and Octet Analysis Studio 13.0 (Sartorius, Göttingen, Germany).

Prior to use, SAX biosensors were prehydrated for 1200 s in assay buffer before use. The optimized assay buffer consisted of 10 mM HEPES, 25 mM NaCl, 0.05% CHAPS, and 0.3% BSA at pH 7.0, selected to minimize NSB while maintaining protein stability. Assays were conducted with orbital shaking at 1000 rpm.

The final assay protocol included five steps: baseline equilibration (180 s), ligand loading (600 s), second baseline (180 s), association (300 s), and dissociation (300 s). Biotinylated HCPs were immobilized at concentrations determined by prior loading scouts to ensure stable capture and reproducible signal. Each interaction was measured across a nine-point, two-fold analyte dilution series ranging from 2 to 533 nM. For each run, unloaded sensors were included to quantify NSB, and ligand-loaded sensors held in buffer served as drift controls.

2.5 | Quantitative Binding Analysis

Sensorgrams obtained from BLI experiments were preprocessed to correct for NSB and baseline drift. This included double referencing using unloaded sensors and buffer blanks, baseline alignment, and interstep correction between assay phases. Two different analytical approaches were applied to evaluate the interactions between HCPs and mAbs: (1) kinetic model fitting and (2) equilibrium response analysis.

2.6 | Kinetic Model Fitting

For interactions with sufficient signal quality, a global 1:1 Langmuir binding model was fitted across multiple analyte concentrations using Octet Analysis Studio 13.0 (Sartorius, Göttingen, Germany). The association rate constant (k_a), dissociation rate constant (k_d), and equilibrium dissociation constant (K_D) were determined from the fits. Only those that met the following predefined quality criteria were included in the analysis: $R^2 > 0.95$, residuals within $\pm 10\%$ of the maximum response, and relative fitting errors $< 10\%$.

2.7 | Equilibrium Response Analysis

For interactions where kinetic model fitting was not feasible due to low signal intensity or non-ideal sensorgram shapes, interaction strength was estimated using the initial slope (S_0) of the Langmuir binding isotherm. Equilibrium response values (R_{eq}) were calculated by averaging the signal over the final 5 s of the association phase across a nine-point analyte concentration series. These values were fitted to a 1:1 Langmuir isotherm, and the initial slope was derived by evaluating the first derivative of the binding curve at low analyte concentrations. The S_0 values were used to rank the relative interaction strength of all mAb and HCP combinations.

2.8 | Validation of BLI Screening Via Protein A Chromatography

To evaluate whether BLI-derived interaction profiles can predict the persistence of HCPs during downstream purification, a Protein A chromatography experiment was performed using PLBL2 as a model HCP. PLBL2 was chosen because it can be quantified using a commercially available ELISA (Tran et al. 2016). In contrast, suitable immunoreagents for direct quantification are currently lacking for the polysorbate-degrading hydrolases investigated in this study (Felix et al. 2025).

PLBL2 was screened against all eight model mAbs using the same BLI assay format and evaluation strategy applied to polysorbate-degrading HCPs. Interaction strength was quantified by equilibrium response analysis and expressed as the initial slope (S_0) of the Langmuir binding isotherm. Based on these results, two antibodies representing high and low interaction profiles (mAb 2 and mAb 6, respectively) were selected for the chromatographic validation experiment.

Protein A chromatography was conducted on an ÄKTA Avant 25 system using MabSelect PrismA resin (Cytiva Life Sciences, Marlborough, USA). Mock harvest material containing native PLBL2 was spiked with either mAb 2 or mAb 6 to achieve a load concentration of 5 mg/mL. The columns were equilibrated using 50 mM Tris–HCl buffer at pH 7.6, loaded at a residence

time of 5 min, washed with three column volumes of equilibration buffer, and eluted with 50 mM sodium acetate buffer at pH 3.5. Fractions from the loading, washing, and elution steps were collected and neutralized immediately after elution.

PLBL2 concentrations in process fractions were quantified as previously described (Weiß et al. 2024). Total HCP clearance was confirmed using Cygnus 3 G anti-CHO HCP antibodies (Southport, North Carolina, USA).

3 | Results

3.1 | Interaction Screening of Polysorbate Degrading HCPs With Monoclonal Antibodies Using BLI

To enable quantitative analysis of HCP–mAb interactions, a BLI-based assay was developed and optimized. The initial evaluation of biosensor formats revealed that Fc-mediated antibody immobilization (ProtA and AHC) and His-tag-based HCP capture (HIS2) were not suitable due to signal instability and high nonspecific binding (Supporting Information Figures 1 and 2). The most robust configuration was achieved using biotinylated HCPs immobilized on streptavidin-coated biosensors, allowing sensitive detection of weak interactions.

This setup was used to systematically screen all combinations between four representative polysorbate degrading HCPs (CES1F, LPLA2, PAF-AH, and PPT1) and eight monoclonal antibodies (mAb 1–8). Figure 1 shows representative sensorgrams for CES1F, illustrating typical association and dissociation behavior across the antibody panel. Most interactions reached equilibrium during the association phase, with signal intensity increasing with analyte concentration and revealing a concentration-dependent specific interaction.

mAb 1, mAb 5, and mAb 7 exhibited the strongest response, while mAb 3 and mAb 6 showed minimal binding, and mAb 8 displayed intermediate signal levels. Comparable interaction patterns were observed for the remaining three polysorbate degrading HCPs (LPLA2, PAF-AH, and PPT1) across the same panel of monoclonal antibodies (Supporting Information Figures 3–5). For each mAb, the overall response trend remained consistent regardless of the HCP, suggesting that all four proteins exhibit a similar transient binding behavior toward the tested mAbs. Nevertheless, absolute differences in signal response were observed. CES1F yielded the highest response, followed by LPLA2, PAF-AH, and PPT1. When comparing sensorgrams, some interactions seem to be biphasic suggesting underlying rebinding effects or heterogeneous binding sites (Figure 1D,E). Biphasic patterns are also seen when comparing the dissociation of mAb 1–mAb 3 since the latter reveals an instant dissociation followed by a second slower dissociation phase (Figure 1A,C). While some sensorgrams appeared biphasic, this may also reflect non-specific adsorption or analyte-analyte interactions at high concentrations. Thus, it is challenging to use a global 1:1 kinetic fitting model to truly describe all interactions.

3.2 | Quantitative Binding Analysis

Two complementary analytical approaches were applied to characterize HCP–mAb interactions: (i) kinetic model fitting based on full association and dissociation phases, and (ii) equilibrium response analysis using steady-state binding levels. Both methods provide affinity estimates and enable a comprehensive assessment of interaction strength. Prior to analysis, all sensorgrams were preprocessed to ensure data quality and comparability. This included double referencing to correct for nonspecific binding and baseline drift.

3.2.1 | *Kinetic Model Fitting*

Kinetic parameters (k_a, k_d, and K_D) were determined by global fitting of a 1:1 Langmuir model using Octet Analysis Studio 13.0 (Sartorius). The model simultaneously estimated the association rate constant (k_a), dissociation rate constant (k_d), and the maximum binding response (R_{max}), with the equilibrium dissociation constant (K_D) calculated as the ratio of k_d–k_a.

Only interaction profiles that met the predefined quality criteria were included in the analysis. These criteria included a clear signal increase during the association phase, a coefficient of determination (R^2) above 0.95, residuals within ± 10% of the maximum response, and relative fitting errors below 10%. Interactions that did not meet these standards were excluded from further evaluation.

Kinetic parameters were successfully determined for five of the eight mAbs across all four HCPs (Table 3). The resulting K_D values span approximately one order of magnitude, ranging from ~40 to ~400 nM. Most interactions showed K_D values between 40 and 90 nM. However, mAb 8 consistently showed higher K_D values, indicating weaker binding. CES1F and LPLA2 exhibited stronger affinities (lower K_D). PPT1 showed slightly weaker interactions.

Across the datasets, association rate constants (k_a) were relatively consistent, typically falling within range of mid to upper hundred-thousands per molar per second. In contrast, dissociation rate constants (k_d) showed greater variability, ranging from low hundredths to nearly two-tenths per second. These observations suggest that the differences in equilibrium dissociation constants (K_D) are primarily driven by variations in complex stability rather than association kinetics. Figure 2 further illustrates this trend, showing the dominant role of dissociation rates in determining overall affinity.

3.2.2 | *Equilibrium Response Analysis*

Equilibrium response analysis was performed to complement kinetic model fitting and to enable the analysis of low affinity interactions (Figure 3). Binding isotherms were generated from steady-state signals across the full analyte concentration range. These isotherms were then fitted to a 1:1 Langmuir model to estimate the apparent K_D values. Although most profiles demonstrated a good fit, saturation was not reached for all mAbs, which limited the reliability of the absolute K_D estimates and a comparison among each other.

To overcome this, the initial slope (S_0) of the binding curve was used as an alternative measure of interaction strength. This approach ensured a quantitative evaluation of all HCP–mAb interactions, including profiles unsuitable for kinetic fitting. Table 4 summarized the initial slope (S_0) values across all HCP–mAb interactions.

Kinetic model fitting was applied to interaction profiles that met stringent quality criteria, resulting in K_D values for five of

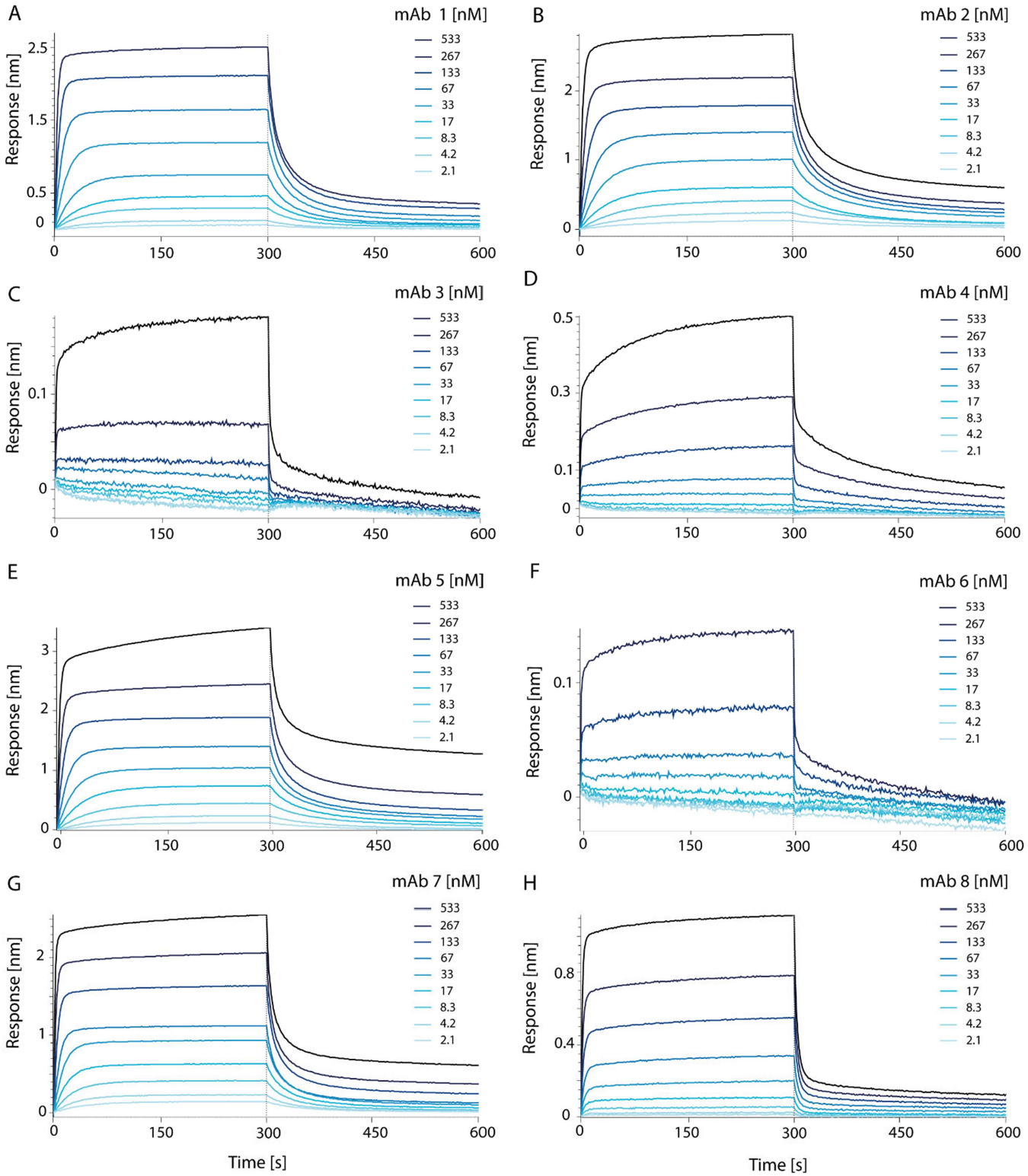

FIGURE 1 | Representative BLI sensorgrams showing the interaction of CES1F with eight monoclonal antibodies. (A) mAb 1; (B) mAb 2; (C) mAb 3; (D) mAb 4; (E) mAb 5; (F) mAb 6; (G) mAb 7; (H) mAb 8. Antibody concentrations ranged from 2 to 533 nM, as indicated by the color legend. Sensorgrams displayed typical association and dissociation phases. Signal intensity increases with antibody concentration and varies between mAbs, reflecting differences in binding behavior while some show biphasic patterns.

the eight mAbs across all four HCPs. In contrast, equilibrium response analysis via S_0 enabled quantification for all mAb–HCP pairs, including those with low-affinity interactions or incomplete saturation, which were unsuitable for kinetic fitting.

To quantify the agreement between the two methods, Spearman's rank correlation coefficient was calculated (Schober et al. 2018). The resulting correlation coefficient ($\rho = 0.9$) indicates a strong agreement between K_D and S_0 ranking, suggesting

TABLE 3 | Kinetic parameters derived from global 1:1 Langmuir fits for HCP–mAb interactions that passed predefined quality criteria. For each interaction, the association rate constant (k_a), dissociation rate constant (k_d), and equilibrium dissociation constant (K_D) are reported. Values represent mean estimates across the tested concentration range. Interactions involving mAb 3, mAb 4, and mAb 6 did not meet quality requirements and are not included.

	mAb	K_D [nM]	k_a [1/Ms]	k_d [1/s]
CES1F	mAb 5	40.16	4.36×10^5	1.75×10^{-2}
	mAb 7	44.02	6.83×10^5	3.01×10^{-2}
	mAb 2	55.01	2.96×10^5	1.63×10^{-2}
	mAb 1	62.48	3.87×10^5	2.42×10^{-2}
	mAb 8	262.30	4.30×10^5	1.13×10^{-1}
PAF-AH	mAb 5	43.03	4.35×10^5	1.87×10^{-2}
	mAb 7	50.56	6.88×10^5	3.48×10^{-2}
	mAb 2	57.83	3.26×10^5	1.89×10^{-2}
	mAb 1	74.78	3.71×10^5	2.77×10^{-2}
	mAb 8	389.08	3.85×10^5	15.00×10^{-2}
PPT1	mAb 5	54.22	4.74×10^5	2.57×10^{-2}
	mAb 2	58.96	3.99×10^5	2.35×10^{-2}
	mAb 7	68.64	6.69×10^5	4.59×10^{-2}
	mAb 1	87.75	4.27×10^5	3.75×10^{-2}
	mAb 8	399.39	4.26×10^5	17.00×10^{-2}
LPLA2	mAb 2	44.75	3.23×10^5	1.44×10^{-2}
	mAb 5	47.51	3.47×10^5	1.65×10^{-2}
	mAb 7	49.01	6.81×10^5	3.34×10^{-2}
	mAb 1	61.86	3.45×10^5	2.14×10^{-2}
	mAb 8	372.80	3.33×10^5	12.40×10^{-2}

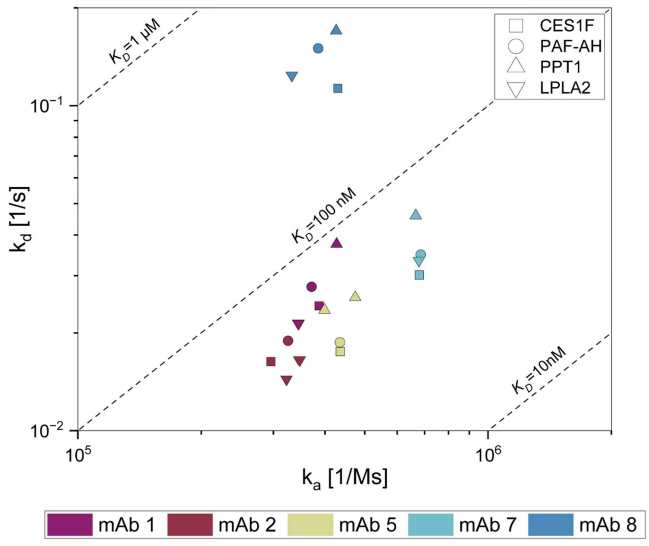

FIGURE 2 | Scatterplot of association rate constant (k_a) vs. dissociation rate constant (k_d) for all HCP–mAb interaction pairs that passed kinetic model fitting quality criteria. Colors indicate the mAb identity (mAb1–mAb8), and symbol shapes indicate the HCP (CES1F, LPLA2, PAF-AH, and PPT1). Dashed iso-K_D lines (10 nM, 100 nM, and 1 μM) are included to visualize affinity levels. The plot illustrates that variation in K_D values across HCP–mAb pairs is primarily driven by differences in dissociation rates (k_d), while association rates (k_a) remain relatively stable.

that equilibrium-based initial slope analysis reliably reflects affinity trends captured by kinetic modeling.

3.3 | Comparative Analysis Across mAbs

For a comparative analysis of mAb interactions across different polysorbate hydrolases, the initial slope of the binding isotherm (S_0) was used as a quantitative descriptor. Since each HCP ligand was immobilized at an individually optimized concentration, absolute S_0 values were not directly comparable. To enable relative comparison across the panel, S_0 values were normalized within each HCP, where 0 represents the weakest interaction and 1 indicates the strongest interaction. The resulting interaction matrix revealed consistent patterns across all HCPs. Ranking the antibodies by their median normalized interaction intensity revealed a clear distinction between those with low and high binding tendencies (Figure 4).

The highest interaction intensities were consistently observed for mAbs 2, 5, and 7, followed by mAb 1 with moderately strong binding. mAb 8 showed intermediate values, while mAbs 6, 3, and 4 exhibited the lowest interaction intensities across the dataset.

To evaluate the contribution of electrostatic properties to interaction strength, the relationship between the theoretical pI and interaction strength was examined (Figure 5). Antibodies with higher pI values generally showed stronger interactions. However, two outliers (mAb 6 and mAb 2) showed the lowest and highest interactions despite having similar pI values. Under

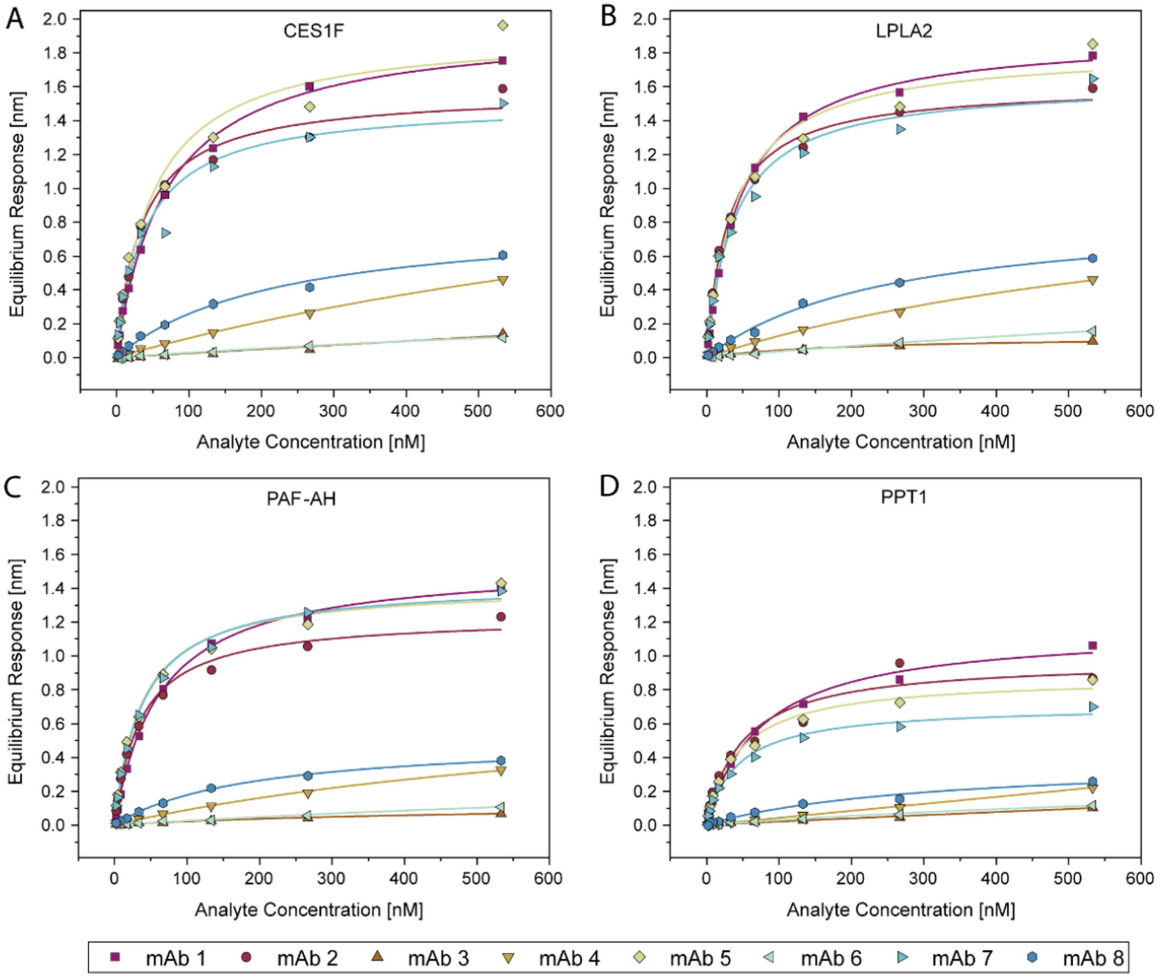

FIGURE 3 | Steady-state binding curves of four polysorbate degrading HCPs CES1F (A), LPLA2 (B), PAF-AH (C), and PPT1 (D) measured across eight monoclonal antibodies (mAbs). For each HCP, equilibrium response values are plotted against increasing analyte concentrations (2–533 nM). Data points indicate experimental measurements, and solid lines represent Langmuir fits assuming a 1:1 binding model.

TABLE 4 | Initial slope values (S_0) derived from Langmuir fits for all HCP–mAb interaction pairs. S_0 reflects the ratio of maximum binding capacity (R_{max}) to dissociation constant (K_D). Values span several orders of magnitude, enabling differentiation between strong and weak binders across the dataset.

	CES1F [nm/nM]	LPLA2 [nm/nM]	PAF-AH [nm/nM]	PPT1 [nm/nM]
mAb 1	2.87×10^{-2}	3.99×10^{-2}	2.49×10^{-2}	1.54×10^{-2}
mAb 2	4.40×10^{-2}	5.31×10^{-2}	3.43×10^{-2}	2.01×10^{-2}
mAb 3	0.02×10^{-2}	0.06×10^{-2}	0.02×10^{-2}	0.02×10^{-2}
mAb 4	0.12×10^{-2}	0.14×10^{-2}	0.10×10^{-2}	0.04×10^{-2}
mAb 5	3.83×10^{-2}	4.41×10^{-2}	3.86×10^{-2}	1.94×10^{-2}
mAb 6	0.03×10^{-2}	0.04×10^{-2}	0.03×10^{-2}	0.03×10^{-2}
mAb 7	3.77×10^{-2}	4.26×10^{-2}	3.67×10^{-2}	1.64×10^{-2}
mAb 8	0.37×10^{-2}	0.34×10^{-2}	0.27×10^{-2}	0.13×10^{-2}

screening conditions, all mAbs carried a net positive charge (pI 7.9–9.6). Theoretical pI values among the polysorbate-degrading HCPs ranged from 6.3 (LPLA2) to 8.6 (PAF-AH), implying that their net charges at pH 7.0 may vary from slightly negative to moderately positive. Based on electrostatic considerations, the strongest attraction would thus be expected for mAb–LPLA2 pairs and the weakest for mAb–PAF-AH. Nevertheless, the observed ranking of mAb binding intensities remained highly consistent across all HCPs (Figure 4), indicating that factors beyond net charge contribute to the observed binding behavior.

Interpretation based on molecule format remains limited because the panel consists mainly of IgG1 antibodies and only two IgG4 antibodies. The two IgG4 molecules showed lower

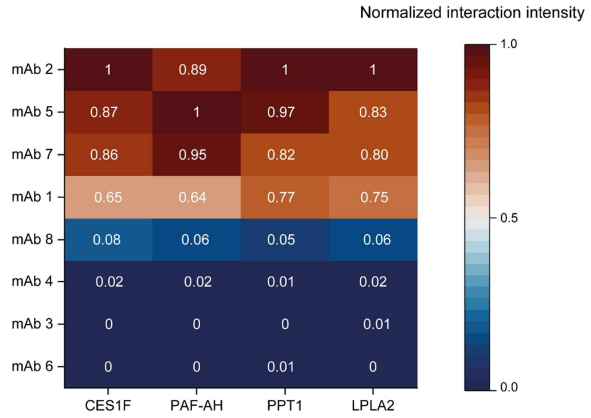

FIGURE 4 | Normalized interaction intensities of monoclonal antibodies with polysorbate hydrolases. The heatmap illustrates the relative binding behavior of eight mAbs across four HCPs (CES1, PAF-AH, PPT1, and LPLA2). Interaction strength is expressed as normalized initial slope values (S_0), where 0 indicates the weakest and 1 the strongest interaction within each ligand. The color scale ranges from deep blue (weak interaction) to dark red (strong interaction), highlighting clear clustering of high-affinity antibodies.

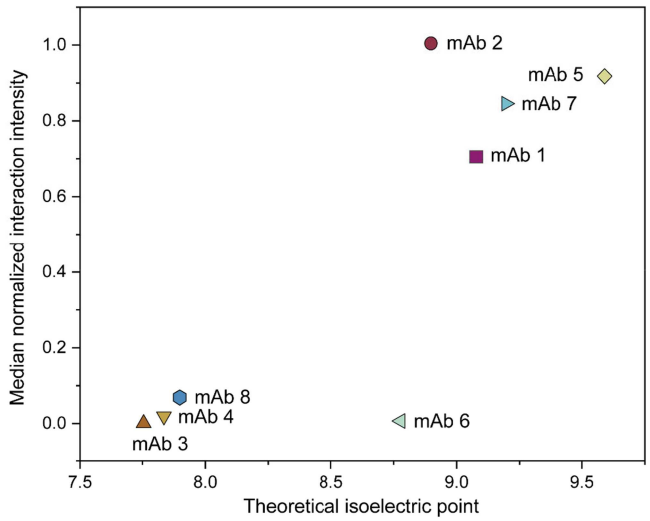

FIGURE 5 | Relationship between theoretical pI and median normalized interaction intensity of mAbs. Each point represents one mAb. Interaction intensity was calculated as the median of normalized initial slope values (S_0) across four polysorbate hydrolases, where 0 indicates the weakest and 1 the strongest interaction. While antibodies with higher pI generally exhibited stronger interactions, outliers deviated from this trend, suggesting that factors beyond net charge contribute to binding behavior.

interaction intensities, however, this result cannot be generalized due to the limited representation of this subclass.

3.4 | Validation of BLI Based Interaction Screening Using Protein A Chromatography

A validation experiment was conducted to evaluate whether BLI-derived interaction profiles can predict HCP persistence during downstream purification. PLBL2 was used as a model HCP. Although PLBL2 is not enzymatically active against polysorbate, it was previously suspected of contributing to polysorbate degradation and remains of interest due to its potential immunogenicity (Zhang et al. 2020). Importantly, PLBL2 is one of the few CHO HCPs for which a commercially available, specific ELISA exists, enabling quantitative analysis across chromatographic fractions.

In contrast, the polysorbate degrading HCPs investigated in this study currently lack commercially available antibodies suitable for ELISA-based quantification (Felix et al. 2025). Therefore, PLBL2 was selected as a representative model to validate whether interaction strength as determined by BLI correlates with impurity carryover in Protein A chromatography.

3.4.1 | *Interaction Profiling of PLBL2*

PLBL2 was screened against all eight model mAbs using the same assay format and evaluation strategy employed for the polysorbate degrading HCPs. Equilibrium response curves were recorded across a nine-point concentration series and analyzed using initial slope (S_0) analysis to quantify interaction intensity (Figure 6).

The resulting profiles showed a wider range of interaction strength compared to the other HCPs. While mAb 2 again showed the highest binding intensity, mAb 6 consistently exhibited the weakest interaction. Interestingly, the relative ranking of some antibodies shifted, for example, mAb 5 and mAb 8.

Based on these results, mAb 2 and mAb 6 were selected for downstream validation.

3.4.2 | *PLBL2 Retention During Protein A Chromatography*

To test whether interaction strength predicts HCP retention, mAb 2 and mAb 6 were spiked into mock harvest material containing native PLBL2. Mock harvest material refers to clarified cell culture supernatant obtained from a non-producing CHO cell line, mimicking the matrix of a typical harvest but without the target mAb. Then, the material was subjected to a standardized Protein A chromatography process. The load, wash and elution fractions were analyzed via ELISA.

Chromatography performance was comparable for both antibodies, with yields above 93% and total HCP clearance close to 99% (Table 5).

Despite similar levels of PLBL2 in the loading material, the eluate of mAb 2 contained approximately 40 ng/mL of PLBL2, while the eluate of mAb 6 only contained about 1 ng/mL (Figure 7A). Fractional analysis revealed that PLBL2 associated with mAb 6 was largely removed during the first wash. In contrast, PLBL2 bound to mAb 2 persisted across the wash and remained present in the eluate (Figure 7B). Overall, these results confirm that stronger BLI-derived interaction signals reflect a higher risk of HCP carryover during purification.

4 | Discussion

The interaction between polysorbate degrading HCPs and monoclonal antibodies represents a critical challenge in biologics development, particularly due to the risk of hitchhiking during downstream processing. While the enzymatic activity of

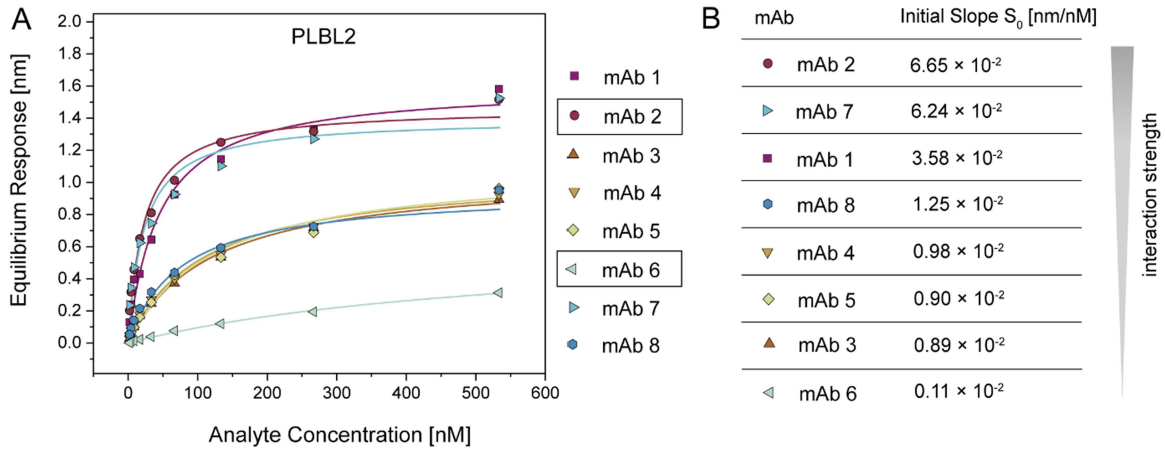

FIGURE 6 | Interaction profiles of PLBL2 with eight monoclonal antibodies. (A) Equilibrium response curves recorded across a nine-point analyte concentration series (2–533 nM) for PLBL2 interactions with different model mAbs. The curves show concentration dependent binding behavior, by varying signal intensities across the antibody panel. (B) Initial slope values (S_0) derived from the equilibrium response data, providing a quantitative measure of interaction strength. The ranking reveals mAb 2 as the strongest binder, while mAb 6 shows the weakest interaction with PLBL2.

TABLE 5 | Yield and overall HCP reduction during Protein A chromatography for mAb 2 and mAb 6.

Parameter	mAb 2	mAb 6
Yield [%]	93.7	94.5
Total HCP reduction [%]	98.9	99.5

polysorbate hydrolases has been extensively characterized, the extent to which weak, reversible protein–protein interactions contribute to their persistence during purification has remained unclear. This study provides a systematic analysis of weak, reversible HCP–mAb interactions and links them to potential hitchhiking behavior during downstream processing.

Using BLI, we observed consistent interaction profiles between several polysorbate hydrolases (CES1F, LPLA2, PAF-AH, and PPT1) and a panel of monoclonal antibodies. These interactions were characterized by equilibrium dissociation constants (K_D) in the low nanomolar range, indicating high apparent affinity. However, the complexes exhibited rapid dissociation ($k_d > 0.01\ s^{-1}$), resulting in a transient binding mode with limited kinetic stability.

Although K_D values were derived using Langmuir fits, saturation was not reached in these assays, likely due to the high analyte concentrations required. In addition, the 1:1 fitting model was not ideal for all mAb interactions as some clearly showed a biphasic behavior revealed by a two-phasic dissociation pattern. However, these heterogeneous binding phenomena may also arise from analyte–analyte interactions or non-specific adsorption at high concentrations, as previously reported for BLI assays (Sherer and Cho 2025). To address this, equilibrium-based descriptors were evaluated as alternatives. The initial slope of the binding isotherm (S_0) correlated well with kinetic rankings and provided complete coverage of all mAbs. As S_0 is proportional to R_{max}/K_D under Langmuir assumptions, it reflects relative affinity even in the absence of saturation.

Compared to previous attempts using SPR or MST, the BLI-based approach demonstrated superior sensitivity for weak, fast-dissociating complexes (Hecht et al. 2022). (Hecht et al. 2022) previously described interactions between LPLA2 and antibodies as "ultra-low affinity" and not detectable using SPR. Similarly, MST failed to detect binding for several enzymes, likely due to the rapid dissociation of these complexes. Our results show that under optimized conditions, BLI can resolve such transient interactions. Several methodological factors likely contribute to this improved sensitivity. First, the use of streptavidin-biotin immobilization on High Precision Streptavidin sensors provided a very stable surface and allows controlled ligand loading, which is essential for weak interaction where even small instabilities can distort the signal (Apiyo 2022; Heiseler et al. 2022). Second, immobilizing biotinylated HCPs and using intact mAbs as analytes increases the optical signal, whereas Fc-capture formats showed baseline drift and high nonspecific binding. Third, the dip-and-read format of BLI avoids fluidics and reduced mass transport limitations that can occur in microfluidic systems, such as SPR (Abdiche et al. 2008; Bates et al. 2025), which might contribute to an improved detection of transient complexes.

The relevance of these findings for downstream processing was demonstrated using PLBL2 as a model HCP. We observed that differences in affinity measured by BLI translated into measurable differences in PLBL2 retention on the Protein A column. Given the transient nature of these interactions, one might expect that both antibody-PLBL2 complexes would be largely removed during the wash steps, resulting in similar clearance levels. Instead, the antibody with higher measured affinity showed higher PLBL2 carryover into the eluate. This indicates that affinity differences directly influence the extent of HCP persistence during the capture step. Our BLI experiments were performed with purified HCPs and mAbs, excluding potential co-purifying species, such as DNA or high molecular weight antibody aggregates. The observed correlation between binding strength and PLBL2 persistence therefore supports direct HCP–mAb binding as a mechanism for hitchhiking. Nevertheless, other studies have shown that DNA-containing complexes or multicomponent aggregates can also promote

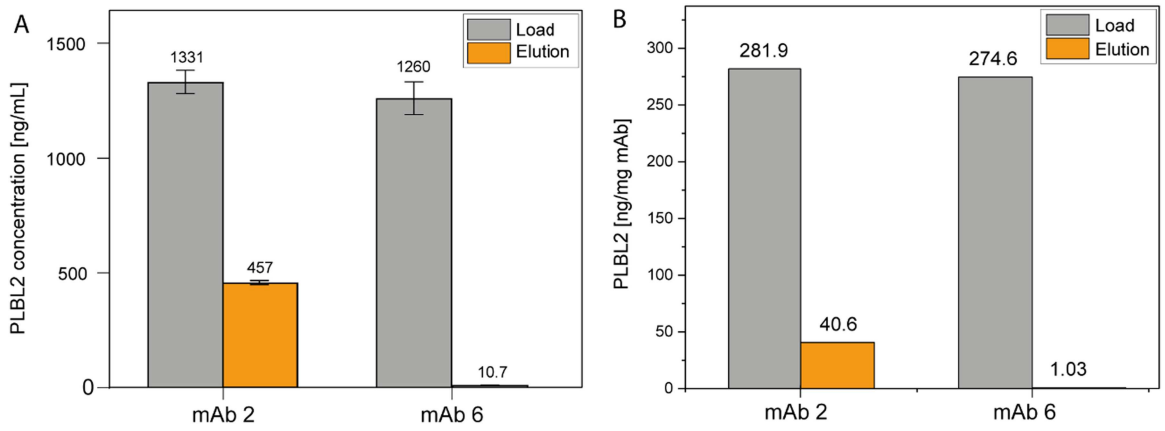

FIGURE 7 | PLBL2 retention during Protein A chromatography for mAb 2 and mAb 6. (A) PLBL2 concentration in load and elution fractions. (B) PLBL2 levels normalized to antibody mass (ng PLBL2 per mg mAb). Both antibodies had comparable PLBL2 in the load, mAb 2 retained higher amounts in the elution compared to mAb 6.

HCP carryover (Bhoyar et al. 2025; Gagnon et al. 2014; Gagnon et al. 2015; Oh et al. 2022). Bhoyar et al. demonstrated that HCP persistence can result from the formation of HCP-antibody aggregates that co-elute during Protein A chromatography (Bhoyar et al. 2025). Similarly, Oh et al. described that HCPs can persist through co-aggregation with unfolded protein response components and chaperones (Oh et al. 2022). In addition, co-elution of HCPs as functional protein networks has been proposed as an independent mechanism contributing to impurity persistence (Luo et al. 2022; Panikulam et al. 2024).

From a process development perspective, the ability to rank antibodies according to their tendency to bind polysorbate degrading HCPs can be a valuable tool for candidate selection. Antibodies with lower binding profiles may carry reduced risk of hitchhiking and associated polysorbate degradation in the final product. Analysis of approved mAbs therapeutics has shown that some HCPs are consistently present, highlighting the importance of product-specific interaction profiles (Molden et al. 2021). Recent studies have shown that molecular descriptors, such as charge distribution, hydrophobicity, and surface accessibility, can predict chromatographic behavior of mAbs (Hess et al. 2024; Maier et al. 2025). Extending these concepts to HCP–mAb interactions may allow quantitative-structure-property relationship (QSPR) models to identify antibodies with lower hitchhiking risk based on sequence or structural features. Integrating BLI-derived experimental data with in-silico predictions could thus enable early-stage risk assessment, supporting both molecule design and purification strategy development. The BLI-assay is also scalable and can be used in a high-throughput format, which makes it a practical tool for screening large numbers of antibodies.

Furthermore, this assay also offers opportunities for structural investigation of HCP–mAb interactions. Fragmentation studies, for example comparing intact mAbs with Fc and Fab fragments, could help localize interaction regions. Similarly, enzymatic deglycosylation of the Fc region could help to clarify if glycosylation patterns contribute to HCP binding, as suggested in previous studies (Hecht et al. 2022).

Complementary approaches, such as site-directed mutagenesis, could further validate structural determinants of interaction (Luo et al. 2022). Computational docking combined with electrostatic and hydrophobic surface mapping has proven effective for identifying potential interaction sites on mAbs and model proteins (Ranjan et al. 2019). Integrating such tools with experimental BLI data could accelerate identification of high-risk regions and inform antibody design for reduced hitchhiking risk.

In summary, our study extends previous observations by directly quantifying interactions between polysorbate-degrading HCPs and mAbs, which were previously considered to be difficult to detect. The data demonstrate that relative affinity differences, even among transient complexes, can translate into measurable differences in HCP persistence during Protein A chromatography.

5 | Conclusion

Our findings describe previous uncharacterized interactions between polysorbate-degrading HCPs and monoclonal antibodies and demonstrate their relevance for downstream processing. These interactions can significantly influence impurity clearance, as shown by differences in HCP retention during Protein A chromatography. The BLI-based approach developed here provides a practical and scalable method to detect and rank such interactions early in development, enabling informed candidate selection to mitigate polysorbate degradation in biopharmaceutical products.

Beyond screening, these insights open opportunities for predictive modeling and structural studies to identify molecular determinants of hitchhiking. Combining experimental interaction profiles with computational descriptors could support rational antibody design and optimized purification strategies.

Ultimately, integrating these concepts into process development can improve control over polysorbate degrading HCPs and enhance overall product quality.

Author Contributions

Melanie Maier: conceptualization, data collection, data analysis and interpretation, writing – original draft, writing – review and editing. **Lukas Griesinger:** data collection, data analysis and interpretation,

writing – review and editing. **Matthias Franzreb:** supervision, writing – review and editing. **Simon Kluters:** conceptualization, supervision, writing – review and editing.

Acknowledgments

We sincerely thank Joey Studts for his continued support of this work. We also thank Linus Weiss and Simon Fischer for valuable discussions and for providing hydrolase overexpression material and mock fermentations used in this study. Finally, we would like to thank Erik Machal for his careful review of the manuscript. This research did not receive any specific grant from funding agencies in the public, commercial, or not-for-profit sectors. This research was wholly funded by Boehringer Ingelheim Pharma GmbH & Co. KG.

Conflicts of Interest

The authors declare no conflicts of interest.

Data Availability Statement

The data that support the findings of this study are available from the corresponding author upon reasonable request.

References

Abdiche, Y., D. Malashock, A. Pinkerton, and J. Pons. 2008. "Determining Kinetics and Affinities of Protein Interactions Using a Parallel Real-Time Label-Free Biosensor, the Octet." *Analytical Biochemistry* 377: 209–217.

Aboulaich, N., W. K. Chung, J. H. Thompson, C. Larkin, D. Robbins, and M. Zhu. 2014. "A Novel Approach to Monitor Clearance of Host Cell Proteins Associated With Monoclonal Antibodies." *Biotechnology Progress* 30: 1114–1124.

Apiyo, D. 2022. *AN-4014: Biomolecular Binding Kinetics Assays on the Octet® BLI Platform*. Sartorius Lab Instruments GmbH & Co. KG.

Bates, T. A., S. K. Gurmessa, J. B. Weinstein, et al. 2025. "Biolayer Interferometry for Measuring the Kinetics of Protein–Protein Interactions and Nanobody Binding." *Nature Protocols* 20: 861–883.

Bhoyar, S., M. Foster, and A. M. Lenhoff. 2025. "Multi-Component Behavior of Host-Cell Protein- and Antibody-Containing Heteroaggregates in Protein A Chromatography." *Journal of Chromatography A* 1753: 465954.

Dwivedi, M., M. Blech, I. Presser, and P. Garidel. 2018. "Polysorbate Degradation in Biotherapeutic Formulations: Identification and Discussion of Current Root Causes." *International Journal of Pharmaceutics* 552: 422–436.

Felix, M. N., T. Waerner, D. Lakatos, B. Reisinger, S. Fischer, and P. Garidel. 2025. "Polysorbates Degrading Enzymes in Biotherapeutics – A Current Status and Future Perspectives." *Frontiers in Bioengineering and Biotechnology* 12: 1490276.

Gagnon, P., R. Nian, J. Lee, et al. 2014. "Nonspecific Interactions of Chromatin With Immunoglobulin G and Protein A, and Their Impact on Purification Performance." *Journal of Chromatography A* 1340: 68–78.

Gagnon, P., R. Nian, Y. Yang, Q. Yang, and C. L. Lim. 2015. "Non-Immunospecific Association of Immunoglobulin G With Chromatin During Elution From Protein A Inflates Host Contamination, Aggregate Content, and Antibody Loss." *Journal of Chromatography A* 1408: 151–160.

Hall, T., S. L. Sandefur, C. C. Frye, T. L. Tuley, and L. Huang. 2016. "Polysorbates 20 and 80 Degradation by Group XV Lysosomal Phospholipase A2 Isomer X1 in Monoclonal Antibody Formulations." *Journal of Pharmaceutical Sciences* 105: 1633–1642.

Hecht, E. S., S. Mehta, A. T. Wecksler, et al. 2022. "Insights Into Ultra-Low Affinity Lipase-Antibody Noncovalent Complex Binding Mechanisms." *mAbs* 14: 2135183.

Heiseler, T., M. Metterlein, G. Calvert, P. Buckle, B. Dass, and L. Bronswijk-Deddens 2022. Optimizing Kinetics Assays to Avoid Avidity Effects. Sartorius Lab Instruments GmbH & Co. KG.

Hess, R., J. Faessler, D. Yun, et al. 2024. "Predicting Multimodal Chromatography of Therapeutic Antibodies Using Multiscale Modeling." *Journal of Chromatography A* 1718: 464706.

Jones, M. T., H.-C. Mahler, S. Yadav, et al. 2018. "Considerations for the Use of Polysorbates in Biopharmaceuticals." *Pharmaceutical Research* 35: 148.

Kerwin, B. A. 2008. "Polysorbates 20 and 80 Used in the Formulation of Protein Biotherapeutics: Structure and Degradation Pathways." *Journal of Pharmaceutical Sciences* 97: 2924–2935.

Kishore, R. S. K., S. Kiese, S. Fischer, A. Pappenberger, U. Grauschopf, and H.-C. Mahler. 2011. "The Degradation of Polysorbates 20 and 80 and Its Potential Impact on the Stability of Biotherapeutics." *Pharmaceutical Research* 28: 1194–1210.

Kovner, D., I. H. Yuk, A. Shen, et al. 2023. "Characterization of Recombinantly-Expressed Hydrolytic Enzymes From Chinese Hamster Ovary Cells: Identification of Host Cell Proteins That Degrade Polysorbate." *Journal of Pharmaceutical Sciences* 112: 1351–1363.

Levy, N. E., K. N. Valente, K. H. Lee, and A. M. Lenhoff. 2016. "Host Cell Protein Impurities in Chromatographic Polishing Steps for Monoclonal Antibody Purification." *Biotechnology and Bioengineering* 113: 1260–1272.

Luo, H., Q. Du, C. Qian, et al. 2022. "Formation of Transient Highly-Charged mAb Clusters Strengthens Interactions With Host Cell Proteins and Results in Poor Clearance of Host Cell Proteins by Protein A Chromatography." *Journal of Chromatography A* 1679: 463385.

Maier, A., M. Cha, S. Burgess, et al. 2025. "Predicting Purification Process Fit of Monoclonal Antibodies Using Machine Learning." *mAbs* 17: 2439988.

Maier, M., S. Schneider, L. Weiss, et al. 2024a. "Tailoring Polishing Steps for Effective Removal of Polysorbate-Degrading Host Cell Proteins in Antibody Purification." *Biotechnology and Bioengineering* 121: 3181–3195.

Maier, M., L. Weiß, N. Zeh, et al. 2024b. "Illuminating a Biologics Development Challenge: Systematic Characterization of CHO Cell-Derived Hydrolases Identified in Monoclonal Antibody Formulations." *mAbs* 16: 2375798.

Molden, R., M. Hu, S. Yen E, et al. 2021. "Host Cell Protein Profiling of Commercial Therapeutic Protein Drugs as a Benchmark for Monoclonal Antibody-Based Therapeutic Protein Development." *mAbs* 13: 1955811.

Oh, Y. H., M. L. Becker, K. M. Mendola, et al. 2022. "Characterization and Implications of Host-Cell Protein Aggregates in Biopharmaceutical Processing." *Biotechnology and Bioengineering* 120: 1068–1080.

Oh, Y. H., K. M. Mendola, L. H. Choe, et al. 2023. "Identification and Characterization of CHO Host-Cell Proteins in Monoclonal Antibody Bioprocessing." *Biotechnology and Bioengineering* 121: 291–305.

Panikulam, S., A. Hanke, F. Kroener, et al. 2024. "Host Cell Protein Networks as a Novel Co-Elution Mechanism During Protein A Chromatography." *Biotechnology and Bioengineering* 121: 1716–1728.

Petersen, R. 2017. "Strategies Using Bio-Layer Interferometry Biosensor Technology for Vaccine Research and Development." *Biosensors* 7: 49.

Ranjan, S., W. K. Chung, M. Zhu, D. Robbins, and S. M. Cramer. 2019. "Implementation of an Experimental and Computational Tool Set to Study Protein-mAb Interactions." *Biotechnology Progress* 35: e2825.

Schober, P., C. Boer, and L. A. Schwarte. 2018. "Correlation Coefficients." *Anesthesia & Analgesia* 126: 1763–1768.

Sherer, N., and J.-H. Cho. 2025. "Overcoming Effects of Heterogeneous Binding on BLI Analysis." *ACS Omega* 10: 28422–28428.

Tran, B., V. Grosskopf, X. Wang, et al. 2016. "Investigating Interactions Between Phospholipase B-Like 2 and Antibodies During Protein A Chromatography." *Journal of Chromatography A* 1438: 31–38.

Tsukidate, T., A. P. Liu, S. Rivera, A. Q. Stiving, J. Welch, and X. Li 2024. Systematic Optimization of Activity-Based Protein Profiling for Identification of Polysorbate-Degradative Enzymes in Biotherapeutic Drug Substance Down to 10 ppb. *bioRxiv*:2024.08.29.610306.

Weiß, L., V. Schmieder-Todtenhaupt, F. Haemmerling, D. Lakatos, P. Schulz, and S. Fischer. 2024. "Multi-Lipase Gene Knockdown in Chinese Hamster Ovary Cells Using Artificial microRNAs to Reduce Host Cell Protein Mediated Polysorbate Degradation." *Biotechnology and Bioengineering* 121: 329–340.

Zhang, S., H. Xiao, M. Goren, et al. 2020. "Putative Phospholipase B-Like 2 Is Not Responsible for Polysorbate Degradation in Monoclonal Antibody Drug Products." *Journal of Pharmaceutical Sciences* 109: 2710–2718.

Supporting Information

Additional supporting information can be found online in the Supporting Information section.
Supplemental Figure 1: Immobilization profiles of His-tagged recombinant HCPs on HIS2 biosensors. **Supplemental Figure 2:** BLI sensorgrams of HCP-mAb interactions using Protein A biosensors. **Supplemental Figure 3:** Representative BLI sensorgrams showing the interaction of LPLA2 with eight monoclonal antibodies. **Supplemental Figure 4:** Representative BLI sensorgrams showing the interaction of PAF-AH with eight monoclonal antibodies. **Supplemental Figure 5:** Representative BLI sensorgrams showing the interaction of PPT1 with eight monoclonal antibodies. **Supplemental Figure 6:** Representative BLI sensorgrams showing the interaction of CES1F with eight monoclonal antibodies. **Supplemental Figure 7:** Representative BLI sensorgrams showing the interaction of PLBL2 with eight monoclonal antibodies.